








Article

Effect of Temperature on the Dynamic Properties of Mixed Surfactant Adsorbed Layers at the Water/Hexane Interface under Low-Gravity Conditions

Volodymyr I. Kovalchuk ^{1,*}, Giuseppe Loglio ^{2,*}, Alexey G. Bykov ³, Michele Ferrari ², Jürgen Krägel ⁴, Libero Liggieri ², Reinhard Miller ^{4,5}, Olga Yu. Milyaeva ³, Boris A. Noskov ³, Francesca Ravera ², Eva Santini ² and Emanuel Schneck ^{4,5}

¹ Institute of Biocolloid Chemistry, 03142 Kyiv (Kiev), Ukraine

² Institute of Condensed Matter Chemistry and Technologies for Energy, Unit of Genoa, 16149 Genoa, Italy; michele.ferrari@ge.icmate.cnr.it (M.F.); libero.liggieri@ge.icmate.cnr.it (L.L.); francesca.ravera@ge.icmate.cnr.it (F.R.); eva.santini@ge.icmate.cnr.it (E.S.)

³ Department of Colloid Chemistry, St. Petersburg State University, 198504 St. Petersburg, Russia; ag-bikov@mail.ru (A.G.B.); o.milyaeva@spbu.ru (O.Y.M.); borisanno@rambler.ru (B.A.N.)

⁴ Max Planck Institute of Colloids and Interface, 14424 Potsdam, Germany; kraegel48@gmail.com (J.K.); miller@fkp.tu-darmstadt.de (R.M.); schneck@fkp.tu-darmstadt.de (E.S.)

⁵ Physics Department, Technical University Darmstadt, 64289 Darmstadt, Germany

* Correspondence: vladim@koval.kiev.ua (V.I.K.); giuseppe.loglio@ge.icmate.cnr.it (G.L.)

Received: 4 June 2020; Accepted: 28 June 2020; Published: 2 July 2020



Abstract: An increase in temperature typically leads to a decrease in the interfacial tension of a water/oil interface. The addition of surfactants to the system can complicate the situation significantly, i.e., the interfacial tension can increase or decrease with an increasing temperature. For most concentrations of the two studied surfactants, the cationic tetradecyl trimethyl ammonium bromide (TTAB) and the nonionic tridecyl dimethyl phosphine oxide (C₁₃DMPO), the measured interfacial tension of the aqueous mixed surfactant solutions against hexane increases when the temperature decreases between 30 °C and 20 °C. However, with a further temperature decrease between 20 °C and 15 °C, the reverse effect has also been observed at some concentrations, i.e., a decrease of interfacial tension. Additionally, the corresponding dilational interfacial visco-elasticity shows some discrepant temperature effects, depending on the bulk concentration and oscillation frequency. The experiments have been performed with a capillary pressure tensiometer under the conditions of micro-gravity. The reason for the positive and negative interfacial tension and visco-elasticity gradients, respectively, within certain ranges of the temperature, concentration and mixing ratios, are discussed on the basis of all available parameters, such as the solubility and partitioning of the surfactants in the two liquid phases and the oscillation frequency.

Keywords: interfacial dilational viscoelasticity; mixed surfactant adsorption layer; water/hexane interface; drop oscillations; capillary pressure tensiometry; effect of temperature; microgravity

1. Introduction

Fundamental knowledge on the adsorption of surfactants at water/oil interfaces is of eminent importance for many technological processes, such as oil recovery [1], food processing [2] and the production of pharmaceuticals and cosmetics [3]. In many cases, surfactant mixtures, rather than single surfactants, are required in order to set up efficient production technologies. The key system parameters for a given water/oil system are the surface activity and bulk concentrations of the used surfactants, their mixing ratio and the temperature [4]. While the impact of surfactant bulk concentrations and the

mixing ratio on the adsorbed amounts is rather easy to explain via the Gibbs fundamental equation [5], the effect of temperature can be quite complicated.

In the literature, there are quite a number of studies on the temperature dependence of surfactant adsorption layers at the water/air interface; however, only very few investigations deal with water/oil interfaces. Typically, the increase in T should result in an increased molar area and consequently in less adsorbed molecules at the interface. This should lead to a decrease in interfacial tension, according to the Gibbs equation. For example, Girifalco and Good discussed this effect in [6] for liquid–solid interfaces. For typical surfactants adsorbed at solution–air interfaces, the impacts of the temperature are quite regular, i.e., with an increasing temperature, the surface tension decreases systematically, as was demonstrated by Chen et al. for n -dodecyl polyoxyethylene glycol monoether with three different oxyethylene chain lengths of 4, 6 and 8 [7]. In contrast, the critical micelle concentration CMC of the studied non-ionic surfactants passes through a minimum in temperature dependence, explained by contributions of enthalpy and entropy to the micellization process, which is balanced at about 50 °C. Das and Das studied the adsorption layers of alkyl trimethyl ammonium bromides (hexadecyl, tetradecyl and dodecyl) at the solution–air interface at temperatures between 25 °C and 50 °C, and they also explained their results on the micellization process in terms of enthalpy–entropy compensation effects without peculiarities [8]. For ionic liquids, the thermodynamics of micelle formation was investigated at temperatures between 5 °C and 55 °C in [9]. The corresponding surface tension isotherms did not show any unexpected temperature effects. For some water–oil systems, however, an opposite trend for interfacial tension changes was observed, i.e., with an increasing temperature, the interfacial tension increased instead of decreasing [10,11]. For mixed surfactant solutions, the temperature dependence of the interfacial tension is much more complex, as discussed by El-Batanoney et al. in [12]. Although investigations on this topic have been published recently [13,14], including Molecular Dynamics simulations [15], many questions could not be answered so far.

Therefore, more measurements on model surfactant solutions at water/oil interfaces are required in order to get some important basic insights into the interfacial behavior. To this end, microgravity conditions are of great importance as they allow for the simplification not only of the experimental measurement conditions but also of the development of new theories for a quantitative description of the interfacial layer behavior [16,17]. More details on the surface/interfacial tension measurements in space can be found, in particular, in ref. [18].

The specific aim of this study is to present an experimental contribution and illustrate the temperature dependence of the interfacial tension and linear dilational viscoelasticity as measured under microgravity conditions with oil drops in aqueous surfactant solutions, subjected to small-amplitude area oscillations. As an oil phase, pure n -hexane was chosen here. The aqueous matrix contained successively injected amounts of the surfactants C_{13} DMPO at a fixed TTAB concentration and of TTAB at a fixed C_{13} DMPO concentration. In these surfactant mixed solutions, the ionic surfactant TTAB is soluble only in the aqueous phase, whereas the non-ionic surfactant C_{13} DMPO is present in both adjacent liquids, according to the corresponding equilibrium partitioning.

2. Materials and Methods

All measurements were performed under microgravity conditions aboard the International Space Station (ISS) by an especially designed instrument, denoted as FASTER (Facility for Adsorption and Surface Tension Research, manufactured by Leonardo S.p.A (formerly Selex-Galileo), Campi Bisenzio, Firenze, Italy). The advantages of microgravity experiments are the possibility of using perfectly spherical shapes of the interface for sufficiently large droplets and the absence of natural convection that usually influences the mass transfer processes in the studied solutions. The instrument is designed as a capillary pressure tensiometer, where the Laplace pressure drop across a curved interface is accurately measured as a function of time by using precise pressure transducers. In this study, a pure n -hexane drop was formed inside an aqueous surfactant solution. The drop was formed at the capillary tip connecting two closed cells filled with the respective liquids. A precise piezo-actuator allows

automatic variation of the drop dimensions (radius of curvature and interfacial area) according to a pre-established timeline. The variation of the interfacial area initiates the relaxation of the interfacial tension, which can be monitored by measuring the Laplace pressure.

The aqueous matrix was a mixture of two surfactants, the non-ionic tridecyl dimethyl phosphine oxide (C_{13} DMPO), (CAS 186953-53-7, purchased from Gamma-Service, Berlin, Germany) and the cationic tetradecyl trimethyl ammonium bromide (TTAB), (CAS 1119-97-7, purchased from Sigma-Aldrich, St. Louis, MO, USA), dissolved in pure MilliQ water. The surfactants were injected step-by-step by using two syringes, working according to a pre-established sequence. The sequence included measurements with increasing C_{13} DMPO concentrations $c_1 = 4.0 \times 10^{-7}, 8.0 \times 10^{-7}, 4.0 \times 10^{-6}, 8.0 \times 10^{-6}$ and 2.2×10^{-5} mol/dm³ at a fixed TTAB concentration of $c_2 = 4.5 \times 10^{-5}$ mol/dm³, continued by measurements with increasing TTAB concentrations $c_2 = 4.5 \times 10^{-5}, 2.2 \times 10^{-4}, 4.5 \times 10^{-4}, 2.2 \times 10^{-3}$ and 4.5×10^{-3} mol/dm³ at a fixed C_{13} DMPO concentration of $c_1 = 2.2 \times 10^{-5}$ mol/dm³.

The selection of the above-mentioned surfactants was motivated by the acquisition of new experimental observations for a typical non-ionic surfactant, soluble in both adjacent liquid phases, in mixture with a typical cationic surfactant. Specifically, C_{13} DMPO was selected due to knowledge gained on it as a single component in previous experimental and theoretical studies [19,20]. TTAB was chosen because of the large knowledge on it as an individual component [21] and because of its favorable Kraft temperature, which is below the available temperature range of the experimental tools. Information about the purity of the two used surfactants is given elsewhere [16].

To obtain information about the interfacial dilational viscoelasticity behavior, harmonic oscillations of the drop interfacial area were generated with eight different frequencies (0.01, 0.02, 0.04, 0.08, 0.16, 0.32, 0.5 and 1.0 Hz, with 12 cycles for each frequency) and three different relative area amplitudes (5%, 10% and 20%). All oscillation experiments were started after 2500 s equilibration time. Additionally, continuously-growing drop experiments were performed for the in-flight pressure sensor calibration adjustment and in-flight CCD-camera calibration, which granted an overall reliability of the obtained results [22]. The measurements were done for three different temperatures ($T = 15$ °C, 20 °C and 30 °C). The work of the pressure sensors (model PDCR-4000, manufactured by GE Druck, Billerica, MA, USA), piezo-actuator (model P-843.40, manufactured by Physik Instrumente GmbH & Co. KG, Karlsruhe, Germany), CCD-camera (model KP-F120F, manufactured by Hitachi Denshi America Ltd., Woodbury, NY, USA) and the other equipment was carefully synchronized.

The data collected from all devices were telemetered according to a pre-established protocol. The obtained equilibrium interfacial tension values were affected by a variable accuracy (i.e., up to ± 0.6 mN m⁻¹), due to occasional push-pull disturbances for the drop caused by the instrumental set parameters. In contrast, the accuracy of the interfacial-viscoelasticity values was much better (i.e., up to ± 0.4 mN m⁻¹) because of the simultaneous appearance of the disturbances of interfacial tension and the corresponding interfacial area. Additional information about the instrument and measurement procedures can be found in [16,22].

3. Theoretical Backgrounds

3.1. Interfacial Tension Measurements

The surfactants dissolved in the aqueous matrix (C_{13} DMPO and TTAB) adsorb at the *n*-hexane/water interface and form a mixed interfacial layer. The resulting interfacial tension is a function of partial surfactant adsorptions (surface concentrations). When the limiting adsorptions (i.e., surface excesses) of two surfactants are not very different, $\Gamma_{1\infty} \approx \Gamma_{2\infty}$, the interfacial tension can be approximately described by Equation (1) [16,23]:

$$\gamma = \gamma_0 + \frac{RT}{\Omega} \ln(1 - \Omega_1 \Gamma_1 - \Omega_2 \Gamma_2) \quad (1)$$

where γ_0 is the interfacial tension of the pure hexane/water interface (about 51.1 mN/m [19,21]), Γ_1 and Γ_2 are the surfactant adsorptions, $\Omega_1 = 1/\Gamma_{1\infty}$ and $\Omega_2 = 1/\Gamma_{2\infty}$ are their molar areas in a densely packed state, and $\Omega = \frac{\Omega_1^2\Gamma_1 + \Omega_2^2\Gamma_2}{\Omega_1\Gamma_1 + \Omega_2\Gamma_2}$ is the average molar area. Under equilibrium conditions, the surfactant adsorptions are functions of their bulk concentrations:

$$\Gamma_j = \Gamma_{j\infty} \frac{b_j^\alpha c_j^\alpha}{1 + b_1^\alpha c_1^\alpha + b_2^\alpha c_2^\alpha}, \quad (j = 1, 2) \quad (2)$$

where C_j^α are the surfactant concentrations in the aqueous matrix (phase α), and b_j^α are their equilibrium adsorption constants. Here and below, the lower indices $j = 1, 2$ are related to the two surfactants, whereas the upper indices α and β are related to the two contacting liquids (water and hexane, respectively). The model, represented by Equations (1) and (2), is one of the simplest models, as it neglects the interactions between the adsorbed molecules, the possible aggregation or reorientation of the adsorbed molecules, and other effects [24].

When two immiscible liquids are in contact, the surfactant molecules can redistribute between them. Under equilibrium conditions, the surfactants' partitioning can be described by the distribution (partition) coefficients, which are the ratios of the surfactant concentrations in the two bulk phases:

$$K_j = \frac{c_j^\beta}{c_j^\alpha}, \quad (j = 1, 2) \quad (3)$$

In the considered case here, the ionic surfactant TTAB is practically not soluble in the oil (*n*-hexane) phase, i.e., its distribution coefficient can be assumed to be zero. However, the non-ionic surfactant C_{13} DMPO is soluble in both liquid phases. In particular, it is more soluble in *n*-hexane, and the respective distribution coefficient is about 30 [20,25].

The latter fact can lead to a small uncertainty in the C_{13} DMPO concentration due to this high solubility in hexane. However, the hexane drop is very small compared to the volume of water in the matrix cell (about 68.2 cm³), and therefore the amount of C_{13} DMPO transferred into the hexane drop is negligibly small. However, the surfactant can diffuse through the capillary (the valve is open during the experiment) to the hexane reservoir (5.6 cm³). The change in the C_{13} DMPO concentration due to this effect should also be relatively small, because the surfactants are injected in continuously increasing amounts and the oscillations are performed shortly after the injections. Therefore, the uncertainty in the C_{13} DMPO concentration should be insignificant [16].

3.2. Interfacial Dilational Viscoelasticity Modulus

The interface response to an imposed dilational area perturbation, $\Delta A(t)$, is the variation of the measured interfacial tension, $\Delta\gamma(t)$. For small-amplitude area perturbations, $\Delta A(t) \ll A_0$, the response of the interface can be characterized by the interfacial dilational viscoelastic modulus:

$$\varepsilon^*(i\omega) = \frac{F\{\Delta\gamma(t)\}}{F\{\Delta A(t)/A_0\}} \quad (4)$$

where F represents the Fourier transform operator of the respective time functions, ω is the variable in the frequency domain (i.e., the angular frequency), and A_0 is the initial interfacial area. From the definition Equation (4), one can see that the interfacial viscoelastic modulus is a complex function of frequency, which can be represented as:

$$\varepsilon^*(i\omega) = \varepsilon_r(\omega) + i\varepsilon_i(\omega) = |\varepsilon^*(i\omega)| \exp[i\varphi(\omega)] \quad (5)$$

where ε_r and ε_i are the real and imaginary parts, respectively, and $|\varepsilon^*(i\omega)|$ and φ are the modulus and phase of the complex viscoelasticity $\varepsilon^*(i\omega)$. In the simplest case of harmonic oscillations, the modulus

$|\varepsilon^*(i\omega)|$ is the ratio of the amplitudes of interfacial tension and relative interfacial area oscillations, whereas the phase φ is the phase shift of interfacial tension with respect to area oscillations.

In the linear approximation, the interfacial dilational viscoelastic modulus, defined by Equation (4), does not depend on the amplitude and the particular shape of the imposed area perturbations as a function of time. Thus, it can be considered as a constitutive property of the interfacial layer [26,27]. Note that the interfacial layer is not an autonomous phase, and that, therefore, the interfacial dilational viscoelastic modulus can depend on the properties of the two contiguous bulk phases [28]. It characterizes the magnitude and the time-scale of the interface response to the external perturbations. This response depends on the time-scale of the relaxation processes within the interfacial system, such as the diffusional exchange of the molecules between the interface and the adjacent liquid bulk phases, the change of structure and morphology of the interfacial layer, the change of orientation and/or conformation of the molecules within the interfacial layer, and/or chemical reactions between the components.

The interpretation of the measured modulus $|\varepsilon^*(i\omega)|$ and phase shift $\varphi(\omega)$ versus frequency dependencies can give access to information about molecular processes occurring in the interfacial system. Accordingly, a number of theoretical models have been developed for the interfacial dilational viscoelasticity modulus in various practical systems [27,29–31]. Particularly worth mentioning are the models for surfactant, polymer, surfactant/polymer or surfactant/protein mixed adsorption layers at the air/water surface [23,32–36]. In previous work [16,17], these models were generalized to the case of a mixture of two surfactants at flat oil/water interfaces and the case of one surfactant at curved oil/water interfaces (i.e., oil-in-water or water-in-oil drops). In the system considered here, both effects (the presence of two surfactants and the curved interface) occur simultaneously, and the respective combined model was presented recently in [37]. According to this model, the interfacial dilational viscoelasticity of a drop interface with a macroscopic (or mesoscopic) radius r_0 can be described by Equation (6):

$$E = \frac{E_{01}}{Z} \left[1 - \frac{a_{12}a_{21}}{a_{11}a_{22}} + W_2 + \frac{\Gamma_{02}}{\Gamma_{01}} \frac{a_{12}}{a_{22}} W_1 \right] + \frac{E_{02}}{Z} \left[1 - \frac{a_{12}a_{21}}{a_{11}a_{22}} + W_1 + \frac{\Gamma_{01}}{\Gamma_{02}} \frac{a_{21}}{a_{11}} W_2 \right] \quad (6)$$

where $Z = (1 + W_1)(1 + W_2) - \frac{a_{12}a_{21}}{a_{11}a_{22}}$, $W_j = \frac{n_j^\alpha r_0 + 1}{(n_j^\alpha)^2 r_0 a_{jj}} + K_j \frac{n_j^\beta r_0 \coth(n_j^\beta r_0) - 1}{(n_j^\beta)^2 r_0 a_{jj}}$ ($j = 1, 2$), $E_{01} = -\left(\frac{\partial \gamma}{\partial \ln \Gamma_1}\right)_{\Gamma_2}$ and $E_{02} = -\left(\frac{\partial \gamma}{\partial \ln \Gamma_2}\right)_{\Gamma_1}$ are the partial elasticities [23], $a_{ji} = \left(\frac{\partial \Gamma_j}{\partial c_i^\alpha}\right)_{c_{k \neq i}^\alpha}$ are the partial derivatives of the adsorptions $\Gamma_1 = \Gamma_1(c_1^\alpha, c_2^\alpha)$ and $\Gamma_2 = \Gamma_2(c_1^\alpha, c_2^\alpha)$ by the surfactants' concentrations c_1^α and c_2^α , Γ_{01} and Γ_{02} are the equilibrium adsorptions, $n_j^\alpha = \sqrt{\frac{i\omega}{D_j^\alpha}}$, $n_j^\beta = \sqrt{\frac{i\omega}{D_j^\beta}}$, and D_j^α and D_j^β are the diffusion coefficients of the surfactants in the outer phase α and inner phase β , respectively. In particular cases, i.e., when either one surfactant is present or a flat interface exists, Equation (6) is reduced to the models discussed in [16,17].

Equation (6) is derived with the assumption of a diffusion limited adsorption mechanism for the two surfactants dissolved in two adjacent liquids. This, particularly, is relevant to microgravity conditions, where surfactant diffusion to/from the interface is not complicated by convection in the bulk. The microgravity conditions also provide a constant value of the curvature radius over the interface for sufficiently large drops and for large density differences between the two liquids.

In our recent work [38], the fractional Maxwell model (FMM), mathematically based on fractional-derivative tools [39–41], was adopted to quantify the observed behavior of the linear interfacial dilational viscoelasticity. It has been shown that the single-element fractional Maxwell model allows the description of the modulus and phase angle of the complex viscoelasticity for a single surfactant system but is not adequate for the case of binary surfactant mixtures. The generalization of this model for systems containing two surfactants is underway.

4. Results and Discussion

4.1. Temperature Dependence of Interfacial Tension

The interfacial tensions measured at three temperatures, $T = 15\text{ }^{\circ}\text{C}$, $20\text{ }^{\circ}\text{C}$ and $30\text{ }^{\circ}\text{C}$, and different surfactant concentrations are shown in Figures 1 and 2. The values presented in these figures are the mean-level values of interfacial tension oscillations measured at each particular frequency. As those, under ideal experimental conditions, they should not depend on frequency as soon as the surfactants' concentrations and the temperatures are fixed. However, because of random disturbances inherent in the intermittent piezo push–pull action (or other disturbances), they slightly vary with the frequency. Nevertheless, in most cases the measured interfacial tensions remain almost constant (within about $\pm 0.5\text{ mN/m}$).

The results presented in Figures 1 and 2 are obtained for drop oscillations with a relative drop area amplitude of about 10%. The results for the amplitudes of 5% and 20% are very similar (more results can be found in the Supplementary Materials, Figures S1 and S2). This indicates an acceptable linearity condition of the interfacial tension responses. Perfect harmonic oscillations of the drop area and an interfacial tension in a wide range of amplitudes of the relative area variations (up to 20%) are advantages of the microgravity environment.

The interfacial tensions generally decrease with increasing surfactant concentrations, except for the two smallest concentrations of C_{13}DMPO in Figure 1. This can be the consequence of incomplete mixing of the solution in the matrix cell after surfactant injections, or of small nitrogen bubbles trapped in the main valve, which might be present at the initial stage of the experiment [16].

The analysis of the temperature dependences shows that the interfacial tensions for the largest temperature, $30\text{ }^{\circ}\text{C}$, are systematically below those for $15\text{ }^{\circ}\text{C}$ and $20\text{ }^{\circ}\text{C}$ (Figures 1 and 2, see also 3D presentation in the Supplementary Materials, Figures S3–S5), in agreement with the usual behavior, i.e., the interfacial tension decreases with an increasing temperature. However, the interfacial tensions for $15\text{ }^{\circ}\text{C}$ and $20\text{ }^{\circ}\text{C}$ do not always show this regularity. In particular, the interfacial tensions for $15\text{ }^{\circ}\text{C}$ are below those for $20\text{ }^{\circ}\text{C}$ for a C_{13}DMPO concentration of $0.4\text{ }\mu\text{m}$ in Figure 1 and for TTAB concentrations of 0.22 mM and 0.45 mM in Figure 2. In the last two cases, the difference between the results for $15\text{ }^{\circ}\text{C}$ and $20\text{ }^{\circ}\text{C}$ is rather small, of about 0.5 mN/m or less. Such a difference is of the same magnitude as the apparent variation of the interfacial tensions with the frequency for fixed surfactant concentrations and temperatures (as discussed above) or with the oscillation amplitude (see the Supporting Information). Thus, the inverse temperature dependences in these two cases can be a consequence of some disturbances of the measurements. For the C_{13}DMPO concentration of $0.4\text{ }\mu\text{m}$ in Figure 1, the difference is larger; however, the results can be affected in this case, probably by incomplete mixing or the effect of small nitrogen bubbles, as discussed above. Therefore, this case cannot be considered as experimental evidence of the inverse temperature dependences either. Unfortunately, the conditions of space experiments do not give the possibility for repeat measurements. Separate accurate experiments should be performed to check the obtained results.

It should be noted that, in the literature, an interfacial tension increase with the temperature is sometimes reported for liquid/liquid systems containing species (surfactants, nano-particles, impurities) capable of adsorbing at the interface [10,42–48]. A non-monotonic variation of the equilibrium surface tension at the air/liquid interface with an increasing temperature was also observed for aqueous solutions of fatty alcohols [49–51]. This effect was later confirmed by specially designed experiments under microgravity conditions [52–54]. A particular consequence of such a non-monotonic variation of the surface tension with the temperature is the specific behavior of “self-wetting fluids” [55–58].

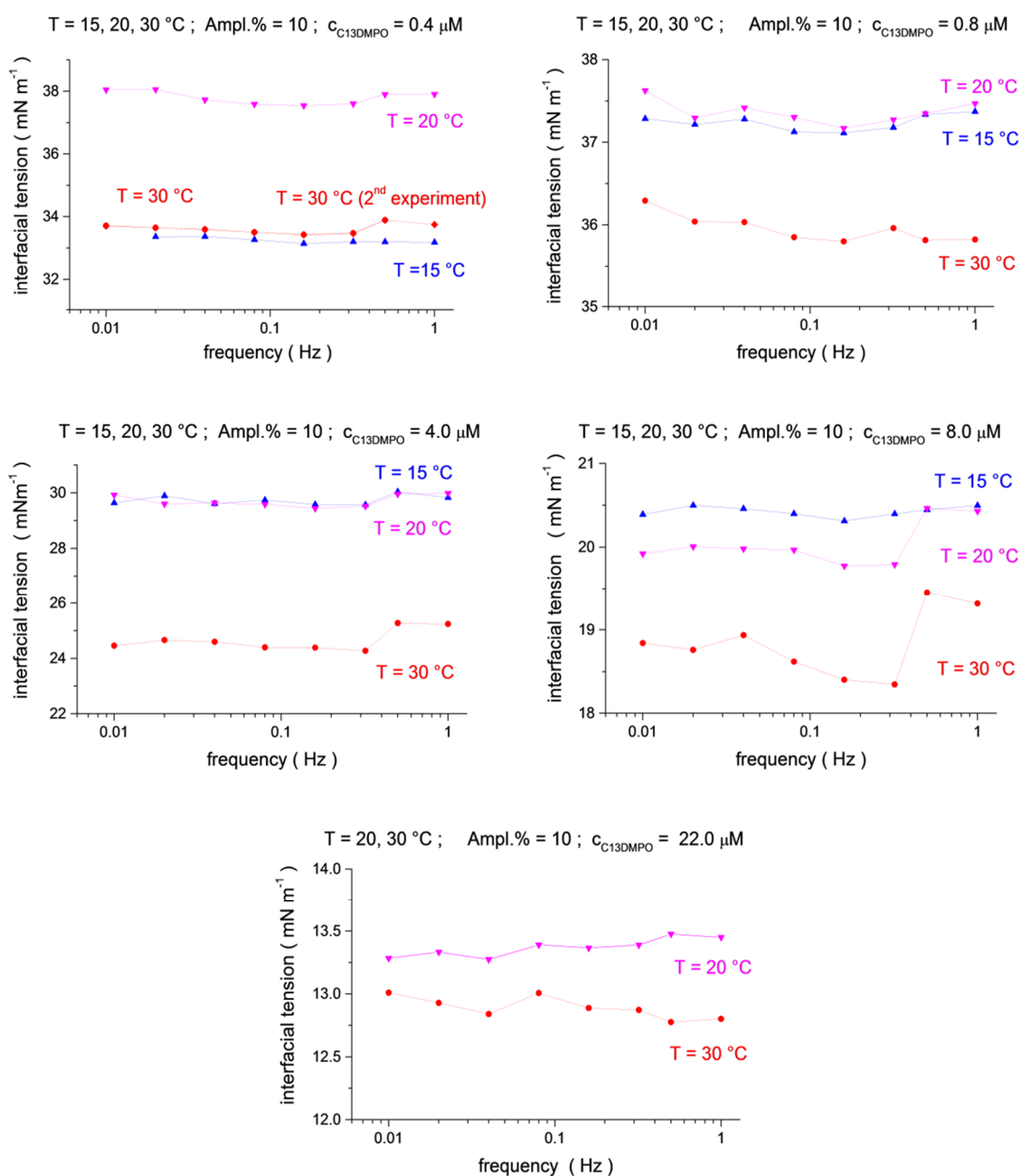


Figure 1. Temperature dependence (blue up triangles T = 15 °C, magenta down triangles T = 20 °C, red circles T = 30 °C) for the mean-level values of interfacial tension oscillations as a function of frequency ($f = 0.01, 0.02, 0.04, 0.08, 0.16, 0.32, 0.5$ and 1.0 Hz) at C₁₃DMPO concentrations of $c_1 = 4.0 \times 10^{-7}, 8.0 \times 10^{-7}, 4.0 \times 10^{-6}, 8.0 \times 10^{-6}$ and 2.2×10^{-5} mol/dm³, and at a fixed TTAB concentration $c_2 = 4.5 \times 10^{-5}$ mol/dm³.

A thermodynamic analysis shows that in multicomponent systems the derivative of interfacial tension with respect to the temperature may be of any sign [59]. However, the molecular mechanisms leading to the increase of interfacial tension with temperature can be different for each particular case and are not always obvious. This can be, in particular, surface or bulk rearrangements [46,49], surfactant aggregation in either of the contacting liquids [10,44], a temperature effect on the surfactants' solubility (and, therefore, on their partition coefficients) [45] or the modification of molecular interactions between the components at the interface [43,47,48]. These factors can influence the form of the equation of state of the adsorption layer and the adsorption isotherms, Equations (1) and (2), or the parameters in

these equations. Furthermore, variations of the partition coefficients can result in changes of surfactant bulk concentrations and adsorptions. All these mechanisms have not been sufficiently studied so far. For the case considered here, the situation appears to be more complicated because the system includes two surfactants, which can behave differently. Moreover, one of them is ionic, and therefore charge effects can also come into play.

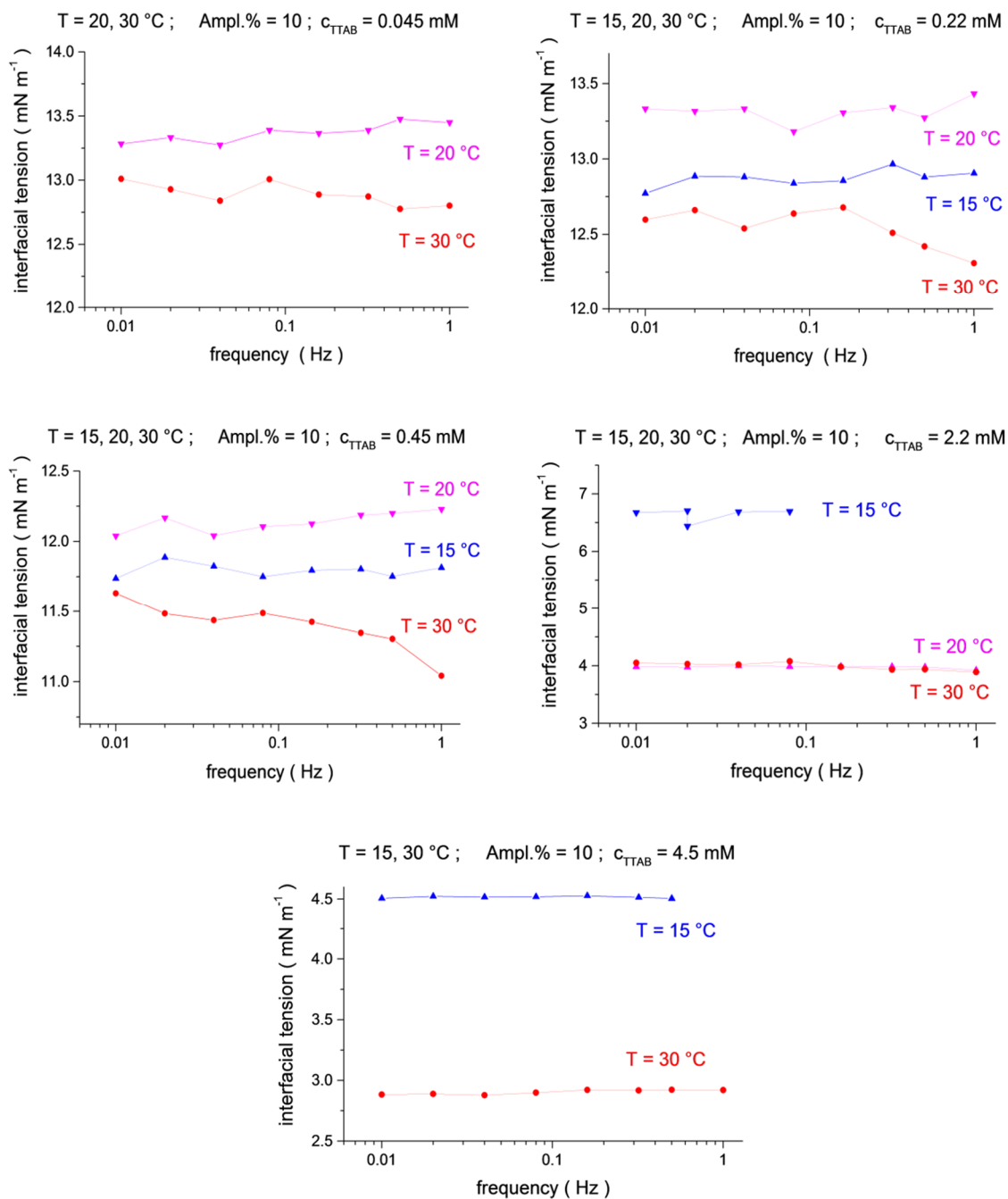


Figure 2. Temperature dependence (blue up triangles T = 15 °C, magenta down triangles T = 20 °C, red circles T = 30 °C) for the mean-level values of interfacial tension oscillations as a function of frequency ($f = 0.01, 0.02, 0.04, 0.08, 0.16, 0.32, 0.5$ and 1.0 Hz) at TTAB concentrations of $c_2 = 4.5 \times 10^{-5}$, 2.2×10^{-4} , 4.5×10^{-4} , 2.2×10^{-3} and 4.5×10^{-3} mol/dm³, at a fixed C₁₃DMPO concentration of $c_1 = 2.2 \times 10^{-5}$ mol/dm³.

4.2. Temperature Dependence of Viscoelastic Modulus

The viscoelastic modulus versus frequency dependencies for three temperatures are shown in Figures 3 and 4 (see also 3D presentation in the Supplementary Materials, Figures S3–S5). One can see that the effect of the temperature depends on the surfactants' concentration. For small concentrations, the modulus shows a clear tendency of decreasing with an increasing temperature (for the two smallest C_{13} DMPO concentrations of 4.0×10^{-7} and 8.0×10^{-7} mol/dm³, and for the smallest TTAB concentration of 4.5×10^{-5} mol/dm³ in Figure 3). However, at higher C_{13} DMPO concentrations (Figure 3) and higher TTAB concentrations (Figure 4), the tendency changes to the opposite—the modulus increases with temperature. The exception to this is the highest TTAB concentration of 4.5×10^{-3} mol/dm³ in Figure 4, where the modulus for 15 °C is again larger than for 30 °C. However, the concentration of 4.5×10^{-3} mol/dm³ is above the CMC for aqueous TTAB solutions (about 3.5×10^{-3} mol/dm³ [60]), so that the mechanisms of the interfacial layer relaxation can be different in this case compared to the lower concentrations. It should also be noted that the magnitude of the modulus is very small in this case (less than 2 mN/m).

Thus, similar to the interfacial tension, the viscoelastic modulus does not exhibit a clear general trend with respect to temperature changes. The variation of the viscoelastic modulus with the temperature can be different depending on the surfactant concentrations and, sometimes, frequencies. Moreover, the viscoelastic modulus behaves differently compared to the interfacial tension, although it definitely depends on it.

Regarding Equation (6), we can see that it includes a number of parameters, which can be divided into two groups. The first group are the parameters that depend only on the equilibrium properties of the adsorption layer and solutions. These are the two partial elasticities, E_{01} and E_{02} , the four partial derivatives of the adsorptions with respect to the concentrations, $a_{ji} = (\partial \Gamma_j / \partial c_i^\alpha)_{c_{k \neq i}^\alpha}$, the two partition coefficients K_1 and K_2 , and the two equilibrium adsorptions Γ_{01} and Γ_{02} . The partial elasticities and the derivatives of the adsorptions with respect to the concentrations can be obtained from the equation of state of the adsorption layer and the adsorption isotherms, such as Equations (1) and (2) or other similar equations. It is clear that, for fixed surfactant concentrations, all these parameters should depend on the temperature, as the respective equations do. However, it is difficult to predict the exact form of this dependence. The partition coefficients and equilibrium adsorptions also vary with the temperature. The second group of parameters are the kinetic coefficients, such as the diffusion coefficients of the surfactants in the two liquid phases, D_j^α and D_j^β , or other kinetic coefficients (if the relaxation of the adsorption layer is not purely diffusion controlled). These kinetic coefficients also strongly depend on the temperature itself and on the liquid's viscosity (the diffusion coefficients, according to the Stokes–Einstein equation). They can also be influenced by the height of the activation barriers (according to the Arrhenius equation), which is affected by the temperature.

Generally, the effect of the diffusion coefficients is that the dependences of the viscoelastic modulus versus frequency should be shifted along the frequency axis. However, in the present case the effect of the diffusion coefficients overlaps with the effect of the partition coefficients and the parameters a_{ji} , which can also lead to complicated shape deformations of these dependences.

This consideration shows that the analysis of temperature dependencies of the viscoelastic modulus is not trivial, as there are so many parameters that can influence the results in a way that is not always predictable. It is clear, however, that the starting point should be the analysis of the temperature dependencies of the equilibrium interfacial tensions for the individual and mixed surfactants solutions. Then, the analysis of the dynamic properties of the interfacial layers will also be much simpler.

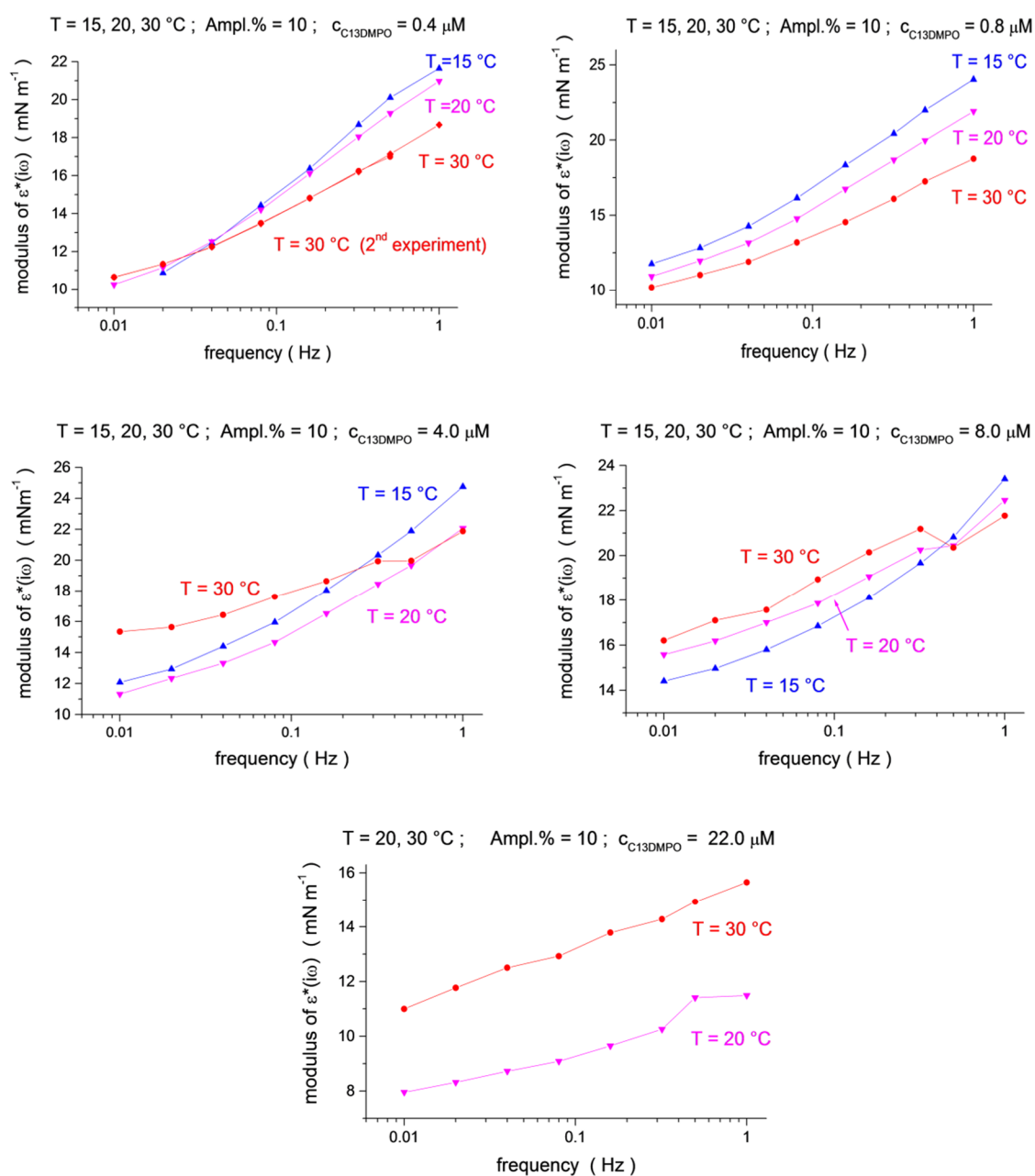


Figure 3. Temperature dependence (blue up triangles $T = 15^\circ\text{C}$, magenta down triangles $T = 20^\circ\text{C}$, red circles $T = 30^\circ\text{C}$) for the $\epsilon^*(i\omega)$ modulus as a function of frequency ($f = 0.01, 0.02, 0.04, 0.08, 0.16, 0.32, 0.5$ and 1.0 Hz) at C_{13}DMPO concentrations of $c_1 = 4.0 \times 10^{-7}, 8.0 \times 10^{-7}, 4.0 \times 10^{-6}, 8.0 \times 10^{-6}$ and 2.2×10^{-5} mol/dm³, at a fixed TTAB concentration of $c_2 = 4.5 \times 10^{-5}$ mol/dm³.

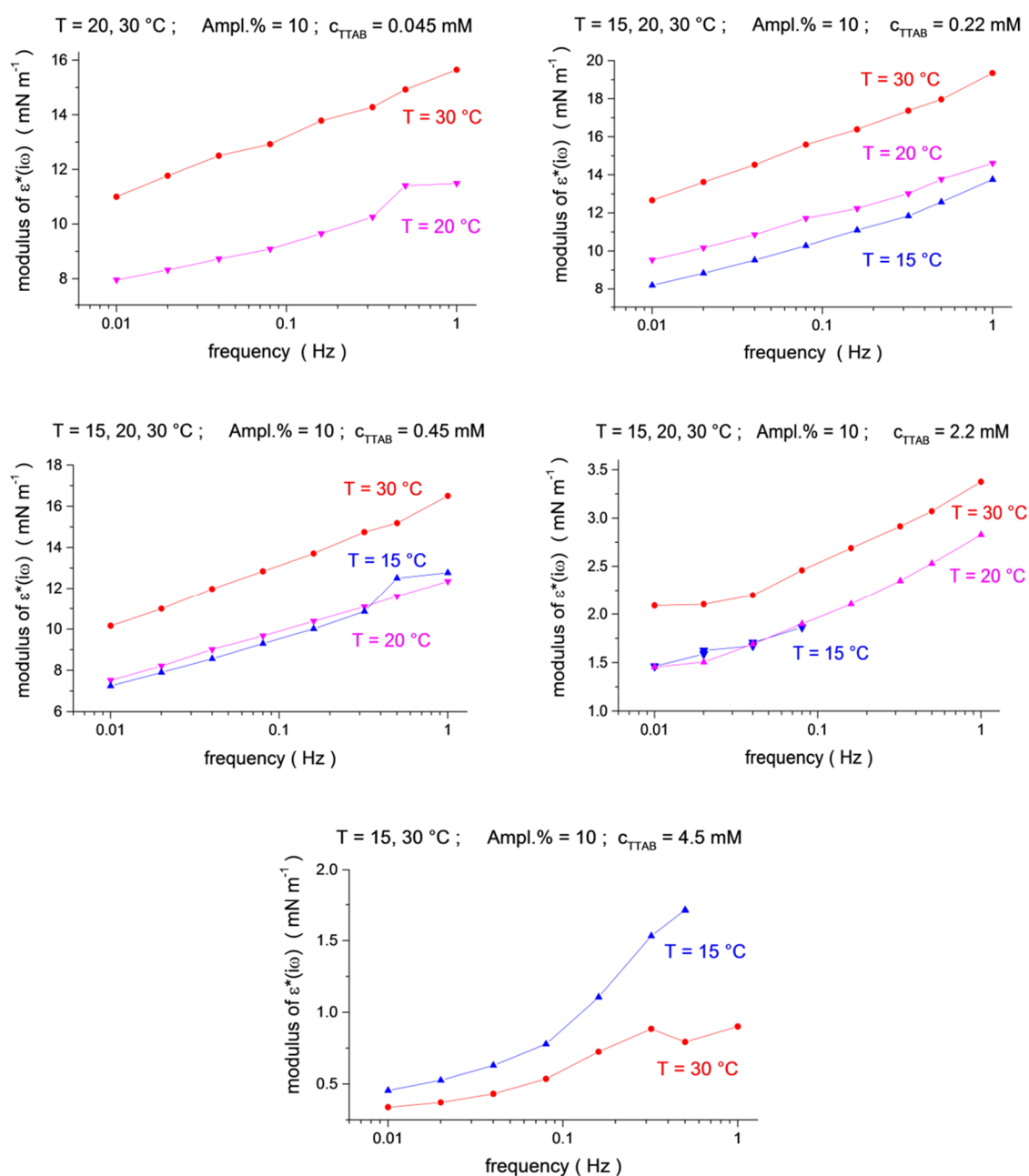


Figure 4. Temperature dependence (blue up triangles T = 15 °C, magenta down triangles T = 20 °C, red circles T = 30 °C) for the $\varepsilon^*(i\omega)$ modulus as a function of frequency ($f = 0.01, 0.02, 0.04, 0.08, 0.16, 0.32, 0.5$ and 1.0 Hz) at TTAB concentrations of $c_2 = 4.5 \times 10^{-5}, 2.2 \times 10^{-4}, 4.5 \times 10^{-4}, 2.2 \times 10^{-3}$ and 4.5×10^{-3} mol/dm³, at a fixed C₁₃DMPO concentration of $c_1 = 2.2 \times 10^{-5}$ mol/dm³.

5. Conclusions

In this study, the interfacial characteristics (interfacial tension and dilational viscoelastic modulus) of the *n*-hexane/water interface were measured for mixed solutions of the non-ionic surfactant C₁₃DMPO and cationic surfactant TTAB. The aim was to determine the temperature effect on the interfacial properties in multi-component liquid systems. This study was part of a wider study performed aboard the International Space Station (ISS) [16,22]. The measurements were done with a special designed instrument. It allows the generation of oscillations of a pure *n*-hexane drop in aqueous matrix solutions. The interfacial tension relaxation served as a response to the drop area oscillations. The microgravity environment allowed for perfect harmonic oscillations of all the system characteristics with sufficiently

high amplitudes (up to 20% of the relative area variations), avoiding natural convection in the solution and drop deformations due to gravity.

The experimental data show that the interfacial tensions at all the concentrations appear in a substantially equilibrium steady (when the mean-level values of the interfacial tension do not change during the oscillations) or quasi-steady (when the mean-level values only change very slowly due to a possible slow redistribution of the surfactants) state. Occasional disturbances are sometimes observed (produced, most probably, by other equipment working in the neighbourhood on the space station). This means that the transient surfactant transfer to or through the interface is, due to its possible slow redistribution in the system, negligibly small compared to the surfactant transfer induced by the drop oscillations. The repetition of the oscillation sequences at different amplitudes can serve as a confirmation of reproducibility of the experimental results and of an acceptable linearity condition of the interfacial tension responses. The measurement method is the well-established capillary pressure method, validated by inflight optical and pressure calibration.

In the temperature interval between 20 °C and 30 °C, the interfacial tension exhibits the usually observed behavior, i.e., it decreases with an increasing temperature. Between 15 °C and 20 °C, at some specific concentrations, the temperature effect on the interfacial tension causes an inverted gradient behavior, instead of the decreasing interfacial tension with an increasing temperature that is typical for pure-liquids. However, these particular results are not sufficient to conclude whether the inverted gradient behavior is really observed in the system that is considered here, as this effect is not sufficiently large and is observed only for few concentrations. Thus, additional accurate experiments should confirm or disprove these results.

Unfortunately, the temperature dependencies of the isotherm parameters and partition coefficients of surfactants in liquid–liquid systems are not yet systematically studied, and even respective data for individual TTAB and C₁₃DMPO in the water/hexane system are not available for comparison. Therefore, the modelling of the temperature dependencies is not possible. However, in this case, experimental data on the temperature dependencies becomes especially valuable, because they can be useful for many practical applications and can be the starting point for further studies in this area.

The temperature effect on the viscoelastic modulus manifests distinguished gradient effects as a function of concentration and frequency, different from the corresponding interfacial tension. The viscoelastic modulus decreases with an increasing temperature for small surfactant concentrations and increases for higher concentrations. The origin of such a behavior of the modulus is not clear. The viscoelastic modulus depends on too many temperature-dependent parameters related to the equilibrium and kinetic properties of the two considered surfactants, capable of dissolving in the two contacting liquids and of adsorbing at the interface. This fact complicates the analysis of temperature effects in the system. The observed phenomenology suggests that one perform new experimental studies on the temperature dependence of the interactions between the components of the mixed adsorption layers and the adjacent liquid phases.

Supplementary Materials: The following are available online at <http://www.mdpi.com/2504-5377/4/3/27/s1>, Figure S1: Temperature (blue T = 15 °C, magenta T = 20 °C, red T = 30 °C) and amplitude (squares—Ampl. 5% up triangles—Ampl. 10%, down triangles—Ampl. 20%) dependences for the mean-level values of interfacial tension oscillations as a function of frequency ($f = 0.01, 0.02, 0.04, 0.08, 0.16, 0.32, 0.5$ and 1.0 Hz) at C₁₃DMPO concentrations of $c_1 = 4.0 \times 10^{-7}, 8.0 \times 10^{-7}, 4.0 \times 10^{-6}, 8.0 \times 10^{-6}$ and 2.2×10^{-5} mol/dm³, and at a fixed TTAB concentration $c_2 = 4.5 \times 10^{-5}$ mol/dm³. Figure S2: Temperature (blue T = 15 °C, magenta T = 20 °C, red T = 30 °C) and amplitude (squares—Ampl. 5%, up triangles—Ampl. 10%, down triangles—Ampl. 20%) dependences for the mean-level values of interfacial tension oscillations as a function of frequency ($f = 0.01, 0.02, 0.04, 0.08, 0.16, 0.32, 0.5$ and 1.0 Hz) at TTAB concentrations of $c_2 = 4.5 \times 10^{-5}, 2.2 \times 10^{-4}, 4.5 \times 10^{-4}, 2.2 \times 10^{-3}$ and 4.5×10^{-3} mol/dm³, at a fixed C₁₃DMPO concentration of $c_1 = 2.2 \times 10^{-5}$ mol/dm³. Figure S3: Temperature dependence (cyan surface T = 20 °C, red surface T = 30 °C) for the mean-level values of interfacial tension oscillations upper panel) and for the $\epsilon^*(i\omega)$ modulus (lower panel) as a function of frequency ($f = 0.01, 0.02, 0.04, 0.08, 0.16, 0.32, 0.5$ and 1.0 Hz) and as a function of concentration, in the concentration sequence for C₁₃DMPO (at concentrations of $4.0 \times 10^{-7}, 8.0 \times 10^{-7}, 4.0 \times 10^{-6}, 8.0 \times 10^{-6}$ and 2.2×10^{-5} mol/dm³ at a fixed TTAB concentration of 4.5×10^{-5} mol/dm³), and of TTAB (at concentrations of $4.5 \times 10^{-5}, 2.2 \times 10^{-4}, 4.5 \times 10^{-4}$ and 2.2×10^{-3} mol/dm³ at a fixed C₁₃DMPO concentration of 2.2×10^{-5} mol/dm³). Graph rotation: Horizontal view = 45°; Vertical view = 15°. Figure S4:

Same as Figure S3. Graph rotation: Horizontal view = 120°; Vertical view = 15°. Figure S5: Same as Figure S3. Graph rotation: Horizontal view = 240°; Vertical view = 15°.

Author Contributions: V.I.K., G.L., A.G.B., M.F., J.K., L.L., R.M., O.Y.M., B.A.N., F.R., E.S. (Eva Santini) and E.S. (Emanuel Schneck) planned the work and designed the experiments; M.F., J.K., G.L., L.L., and R.M. conducted the microgravity experiments; V.I.K. and G.L. performed the elaboration of the telemetered data; V.I.K., G.L., and R.M. interpreted and discussed the data; V.I.K., G.L., and R.M. wrote the manuscript. All authors have read and agreed to the published version of the manuscript.

Funding: European Space Agency MAP Projects “Soft Matter Dynamics”, “Emulsion Dynamics and Droplet Interfaces - EDDI”, “Fundamental and Applied Studies in Emulsion Stability - FASES”. European Space Agency Project “Particle Stabilized Emulsions - PASTA” (AO-2009-0813) (and the corresponding grants by the Italian Space Agency ASI n. 2013-028-R.O).

Acknowledgments: We are grateful to Piero Pandolfini for his contribution in the elaboration of the telemetered data.

Conflicts of Interest: The authors declare no conflict of interest.

References

1. Iglauer, S.; Favretto, S.; Spinosa, G.; Schena, G.; Blunt, M.J. X-ray tomography measurements of power-law cluster size distributions in sandstones. *Phys. Rev. E* **2010**, *82*, 056315. [[CrossRef](#)] [[PubMed](#)]
2. Fredrick, E.; Walstra, P.; Dewettinck, K. Factors governing partial coalescence in oil-in-water emulsions. *Adv. Colloid Interface Sci.* **2010**, *153*, 30–42. [[CrossRef](#)] [[PubMed](#)]
3. Gonçalves, L.M.; Kobayakawa, T.G.; Zanette, D.; Chaimovich, H.; Cuccovia, I.M. Effects of micelles and vesicles on the oximolysis of p-nitrophenyl diphenyl phosphate: A model system for surfactant-based skin-defensive formulations against organophosphates. *J. Pharm. Sci.* **2009**, *98*, 1040–1052. [[CrossRef](#)] [[PubMed](#)]
4. Al-Sahhaf, T.; Elkamel, A.; Suttar Ahmed, A.; Knan, A.R. The influence of temperature, pressure, salinity, and surfactant concentration on the interfacial tension of the *n*-octane-water system. *Chem. Eng. Comm.* **2005**, *192*, 667–684. [[CrossRef](#)]
5. He, Y.; Yazhgur, P.; Salonen, A.; Langevin, D. Adsorption–desorption kinetics of surfactants at liquid surfaces. *Adv. Colloid Interf. Sci.* **2015**, *222*, 377–384. [[CrossRef](#)]
6. Girifalco, L.A.; Good, R.J. A theory for the estimation of surface and interfacial energies. Derivation and application to interfacial tension. *J. Phys. Chem.* **1957**, *61*, 904–909. [[CrossRef](#)]
7. Chen, L.J.; Lin, S.Y.; Huang, C.C.; Chen, E.M. Temperature dependence of critical micelle concentration of polyoxyethylenated non-ionic surfactants. *Colloids Surf. A* **1998**, *135*, 175–181. [[CrossRef](#)]
8. Das, C.; Das, B. Thermodynamic and Interfacial Adsorption Studies on the Micellar Solutions of Alkyltrimethylammonium Bromides in Ethylene Glycol (1) + Water (2) Mixed Solvent Media. *J. Chem. Eng. Data* **2009**, *54*, 559–565. [[CrossRef](#)]
9. Geng, F.; Liu, J.; Zheng, L.; Yu, L.; Li, Z.; Li, G.; Tung, C. Micelle Formation of Long-Chain Imidazolium Ionic Liquids in Aqueous Solution Measured by Isothermal Titration Microcalorimetry. *J. Chem. Eng. Data* **2010**, *55*, 147–151. [[CrossRef](#)]
10. Aveyard, R.; Binks, B.P.; Chen, J.; Esquena, J.; Fletcher, P.D.I.; Buscall, R.; Davies, S. Surface and Colloid Chemistry of Systems Containing Pure Sugar Surfactant. *Langmuir* **1998**, *14*, 4699–4709. [[CrossRef](#)]
11. Aoudia, M.; Al-Shibli, M.N.; Al-Kasimi, L.H.; Al-Maamari, R.; Al-Bemani, A. Novel surfactants for ultralow interfacial tension in a wide range of surfactant concentration and temperature. *J. Surfactant Deterg.* **2006**, *9*, 287–293. [[CrossRef](#)]
12. El-Batanoney, M.; Abdel-Moghny, T.; Ramzi, M. The effect of mixed surfactants on enhancing oil recovery. *J. Surfactant Deterg.* **1999**, *2*, 201–205. [[CrossRef](#)]
13. Fu, D.; Gao, X.R.; Huang, B.; Wang, J.; Sun, Y.; Zhang, W.J.; Kan, K.; Zhang, X.C.; Xie, Y.; Sui, X. Micellization, surface activities and thermodynamics study of pyridinium-based ionic liquid surfactants in aqueous solution. *RSC Adv.* **2019**, *9*, 28799–28807. [[CrossRef](#)]
14. Szymczyk, K.; Szaniawska, M.; Krawczyk, J. Temperature Effect on the Adsorption and Volumetric Properties of Aqueous Solutions of Kolliphor®ELP. *Molecules* **2020**, *25*, 743. [[CrossRef](#)] [[PubMed](#)]
15. Ivanova, A.A.; Cheremisin, A.N.; Barifcani, A.; Iglauer, S.; Phan, C. Molecular insights in the temperature effect on adsorption of cationic surfactants at liquid/liquid interfaces. *J. Mol. Liq.* **2020**, *299*, 112104. [[CrossRef](#)]

16. Loglio, G.; Kovalchuk, V.I.; Bykov, A.G.; Ferrari, M.; Krägel, J.; Liggieri, L.; Miller, R.; Noskov, B.A.; Pandolfini, P.; Ravera, F.; et al. Dynamic properties of mixed cationic/nonionic adsorbed layers at the *n*-hexane/water interface: Capillary pressure experiments under low gravity conditions. *Colloids Interfaces* **2018**, *2*, 53. [[CrossRef](#)]
17. Kovalchuk, V.I.; Aksenenko, E.V.; Makievski, A.V.; Fainerman, V.B.; Miller, R. Dilational interfacial rheology of tridecyl dimethyl phosphine oxide adsorption layers at the water/hexane interface. *J. Colloid Interf. Sci.* **2019**, *539*, 30–37. [[CrossRef](#)]
18. Passerone, A. Twenty Years of Surface Tension Measurements in Space. *Microgravity Sci. Technol.* **2011**, *23*, 101–111. [[CrossRef](#)]
19. Ferrari, M.; Liggieri, L.; Ravera, F.; Amodio, C.; Miller, R. Adsorption kinetics of alkyl phosphine oxides at the water/hexane interface 1. Pendant drop experiments. *J. Colloid Interface Sci.* **1997**, *186*, 40–45. [[CrossRef](#)]
20. Liggieri, L.; Ravera, F.; Ferrari, M.; Passerone, A.; Miller, R. Adsorption Kinetics of alkyl phosphine oxides at water/hexane interface 2. Theory of the adsorption with transport across the interface in finite systems. *J. Colloid Interface Sci.* **1997**, *186*, 46–52. [[CrossRef](#)]
21. Mucic, N.; Kovalchuk, N.M.; Pradines, V.; Javadi, A.; Aksenenko, E.V.; Krägel, J.; Miller, R. Dynamic properties of C_nTAB adsorption layers at the water/oil interface. *Colloids Surf. A* **2014**, *441*, 825–830. [[CrossRef](#)]
22. Pandolfini, P.; Loglio, G.; Ravera, F.; Liggieri, L.; Kovalchuk, V.I.; Javadi, A.; Karbaschi, M.; Krägel, J.; Miller, R.; Noskov, B.A.; et al. Dynamic properties of Span-80 adsorbed layers at paraffin–oil/water interface: Capillary pressure experiments under low gravity conditions. *Colloids Surf. A Phys. Eng. Asp.* **2017**, *532*, 228–243. [[CrossRef](#)]
23. Joos, P. *Dynamic Surface Phenomena*; VSP: Dordrecht, The Netherlands, 1999.
24. Fainerman, V.B.; Miller, R.; Aksenenko, E.V.; Makievski, A.V. Equilibrium Adsorption Properties of Single and Mixed Surfactant Solutions. In *Surfactants Chemistry, Interfacial Properties, Applications, Studies in Interface Science*; Fainerman, V.B., Möbius, D., Miller, R., Eds.; Elsevier: Amsterdam, The Netherlands, 2001; Volume 13, chapter 3.
25. Fainerman, V.B.; Sharipova, A.A.; Aidarova, S.B.; Kovalchuk, V.I.; Aksenenko, E.V.; Makievski, A.V.; Miller, R. Direct determination of the distribution coefficient of tridecyl dimethyl phosphine oxide between water and hexane. *Colloids Interfaces* **2018**, *2*, 28. [[CrossRef](#)]
26. Loglio, G.; Tesei, U.; Cini, R. Spectral Data of Surface Viscoelastic Modulus Acquired via Digital Fourier Transformation. *J. Colloid Interface Sci.* **1979**, *71*, 316–320. [[CrossRef](#)]
27. Miller, R.; Liggieri, L. *Interfacial Rheology*, 1st ed.; CRC Press: Boca Raton, FL, USA, 2009; Volume 1, pp. 1–37.
28. Defay, R.; Prigogine, I.; Sanfeld, A. Surface thermodynamics. *J. Colloid Interface Sci.* **1977**, *58*, 498–510. [[CrossRef](#)]
29. Noskov, B.A.; Loglio, G. Dynamic surface elasticity of surfactant solutions. *Colloids Surf. A* **1998**, *143*, 167–183. [[CrossRef](#)]
30. Ivanov, I.B.; Danov, K.D.; Ananthapadmanabhan, K.P.; Lips, A. Interfacial rheology of adsorbed layers with surface reaction: On the origin of the dilatational surface viscosity. *Adv. Colloid Interface Sci.* **2005**, *114*, 61–92. [[CrossRef](#)]
31. Ravera, F.; Ferrari, M.; Liggieri, L. Modelling of dilational visco-elasticity of adsorbed layers with multiple kinetic processes. *Colloids Surf. A* **2006**, *282*, 210–216. [[CrossRef](#)]
32. Jiang, Q.; Valentini, J.E.; Chiew, Y.C. Theoretical models for dynamic dilational surface properties of binary surfactant mixtures. *J. Colloid Interface Sci.* **1995**, *174*, 268–271. [[CrossRef](#)]
33. Noskov, B.A. Dynamic surface elasticity of polymer solutions. *Colloid Polym. Sci.* **1995**, *273*, 263–270. [[CrossRef](#)]
34. Aksenenko, E.V.; Kovalchuk, V.I.; Fainerman, V.B.; Miller, R. Surface dilational rheology of mixed adsorption layers at liquid interfaces. *Adv. Colloid Interface Sci.* **2006**, *122*, 57–66. [[CrossRef](#)] [[PubMed](#)]
35. Aksenenko, E.V.; Kovalchuk, V.I.; Fainerman, V.B.; Miller, R. Surface dilational rheology of mixed surfactants layers at liquid interface. *J. Phys. Chem. C* **2007**, *111*, 14713–14719. [[CrossRef](#)]
36. Liu, F.; Darjani, S.; Akhmetkhanova, N.; Maldarelli, C.; Banerjee, S.; Pauchard, V. Mixture Effect on the Dilatation Rheology of Asphaltenes-Laden Interfaces. *Langmuir* **2017**, *33*, 1927–1942. [[CrossRef](#)] [[PubMed](#)]
37. Bykov, A.G.; Ferrari, M.; Kovalchuk, V.I.; Krägel, J.; Liggieri, L.; Loglio, G.; Makievski, A.V.; Miller, R.; Milyaeva, O.Y.; Noskov, B.A.; et al. The surface dilational viscoelasticity of a curved oil-water interface with two surfactants soluble in both the oil and water phase. In *Proceedings of the 8th Bubble and Drop Conference (B&D 2019)*, Sofia, Bulgaria, 24–28 June 2019.

38. Loglio, G.; Kovalchuk, V.I.; Bykov, A.G.; Ferrari, M.; Krägel, J.; Liggieri, L.; Miller, R.; Noskov, B.A.; Pandolfini, P.; Ravera, F.; et al. Interfacial Dilational Viscoelasticity of Adsorption Layers at the Hydrocarbon/Water Interface: The Fractional Maxwell Model. *Colloids Interfaces* **2019**, *3*, 66. [[CrossRef](#)]
39. Costa, M.F.P.; Ribeiro, C. Generalized fractional Maxwell model: Parameter estimation of a viscoelastic material. *AIP Conf. Proc.* **2012**, *1479*, 790–793. [[CrossRef](#)]
40. Stankiewicz, A. Fractional Maxwell model of viscoelastic biological materials. *BIO Web Conf.* **2018**, *10*, 02032. [[CrossRef](#)]
41. Povstenko, Y. Essentials of fractional calculus. In *Fractional Thermoelasticity*; Springer International Publishing: Basel, Switzerland, 2015; Volume 219. [[CrossRef](#)]
42. Lutton, E.S.; Stauffer, C.E.; Martin, J.B.; Fehl, A.J. Solid and liquid monomolecular film at oil/H₂O interfaces. *J. Colloid Interface Sci.* **1969**, *30*, 283–290. [[CrossRef](#)]
43. Ataev, G.M. Anomalous Temperature Dependence of Interfacial Tension in Water–Hydrocarbon Mixtures. *Russ. J. Phys. Chem.* **2007**, *81*, 2094–2095. [[CrossRef](#)]
44. Ye, Z.; Zhang, F.; Han, L.; Luo, P.; Yang, J.; Chen, H. The effect of temperature on the interfacial tension between crude oil and gemini surfactant solution. *Colloids Surf. A* **2008**, *322*, 138–141. [[CrossRef](#)]
45. Miquilena, A.; Coll, V.; Borges, A.; Melendez, J.; Zeppieri, S. Influence of Drop Growth Rate and Size on the Interfacial Tension of Triton X-100 Solutions as a Function of Pressure and Temperature. *Int. J. Thermophys.* **2010**, *31*, 2416–2424. [[CrossRef](#)]
46. Ferdous, S.; Ioannidis, M.A.; Henneke, D.E. Effects of temperature, pH, and ionic strength on the adsorption of nanoparticles at liquid–liquid interfaces. *J. Nanopart. Res.* **2012**, *14*, 850. [[CrossRef](#)]
47. Hyde, A.; Horiguchi, M.; Minamishima, N.; Asakuma, Y.; Phan, C. Effects of microwave irradiation on the decane-water interface in the presence of Triton X-100. *Colloids Surf. A* **2017**, *524*, 178–184. [[CrossRef](#)]
48. Shibata, Y.; Hyde, A.; Asakuma, Y.; Phan, C. Thermal response of a non-ionic surfactant layer at the water/oil interface during microwave heating. *Colloids Surf. A* **2018**, *556*, 127–133. [[CrossRef](#)]
49. Vochten, R.; Petre, G. Study of the heat of reversible adsorption at the air-solution interface. II. Experimental determination of the heat of reversible adsorption of some alcohols. *J. Colloid Interface Sci.* **1973**, *42*, 320–327. [[CrossRef](#)]
50. Petre, G.; Azouni, M.A. Experimental evidence for the minimum of surface tension with temperature at aqueous alcohol solution air interfaces. *J. Colloid Interface Sci.* **1984**, *98*, 261–263. [[CrossRef](#)]
51. Slavtchev, S.G.; Miladinova, S.P. Thermocapillary flow in a liquid layer at minimum in surface tension. *Acta Mech.* **1998**, *127*, 209–224. [[CrossRef](#)]
52. Legros, J.C.; Limbourg-Fontaine, M.C.; Petre, G. Influence of a surface tension minimum as a function of temperature on the Marangoni convection. *Acta Astronaut.* **1984**, *11*, 143–147. [[CrossRef](#)]
53. Limbourg-Fontaine, M.C.; Petre, G.; Legros, J.C. Thermocapillary movements under at a minimum of surface tension. *Naturwissenschaften* **1986**, *73*, 360–362. [[CrossRef](#)]
54. Savino, R.; Cecere, A.; Vaerenbergh, S.V.; Abe, Y.; Pizzirusso, G.; Tzevelecos, W.; Mojahed, M.; Galand, Q. Some experimental progresses in the study of the self-rewetting fluids for the SELENE experiment to be carried in the Thermal Platform 1 hardware. *Acta Astronaut.* **2013**, *89*, 179–188. [[CrossRef](#)]
55. Savino, R.; Cecere, A.; Paola, R.D. Surface tension driven flow in wickless heat pipes with self-rewetting fluids. *Int. J. Heat Fluid Flow* **2009**, *30*, 380–388. [[CrossRef](#)]
56. Karapetsas, G.; Sahu, K.C.; Sefiane, K.; Matar, O.K. Thermocapillary-Driven Motion of a Sessile Drop: Effect of Non-Monotonic Dependence of Surface Tension on Temperature. *Langmuir* **2014**, *30*, 4310–4321. [[CrossRef](#)]
57. Tripathi, M.K.; Sahu, K.C.; Karapetsas, G.; Sefiane, K.; Matar, O.K. Non-isothermal bubble rise: Non-monotonic dependence of surface tension on temperature. *J. Fluid Mech.* **2015**, *763*, 82–108. [[CrossRef](#)]
58. Balla, M.; Tripathi, M.K.; Sahu, K.C.; Karapetsas, G.; Matar, O.K. Non-isothermal bubble rise dynamics in a self-rewetting fluid: Three-dimensional effects. *J. Fluid Mech.* **2019**, *858*, 689–713. [[CrossRef](#)]
59. Rusanov, A.I.; Prokhorov, V.A. Interfacial tensiometry. In *Studies in Interface Science*; Elsevier: Amsterdam, The Netherlands, 1996; Volume 3, Chapter 1.
60. Bergeron, V. Disjoining Pressures and Film Stability of Alkyltrimethylammonium Bromide Foam Films. *Langmuir* **1997**, *13*, 3474–3482. [[CrossRef](#)]

